CORTEX 127 (2020) 231–247

Available online at www.sciencedirect.com

ScienceDirect

Journal homepage: www.elsevier.com/locate/cortex

Special Issue "The Neuropsychology of Unwanted Thoughts and Actions": Research Report

Common neuronal mechanisms underlying tics and hyperactivity

*Michal Israelashvili, Dorin Yael, Esther Vinner, Katya Belelovsky and Izhar Bar-Gad**

The Leslie & Susan Goldschmied (Gonda) Multidisciplinary Brain Research Center, Bar-Ilan University, Ramat-Gan, Israel

ARTICLE INFO

Article history:
Received 4 August 2019
Reviewed 22 September 2019
Revised 17 November 2019
Accepted 4 February 2020
Published online 29 February 2020

Keywords:
Tourette syndrome
Attention deficit hyperactivity disorder (ADHD)
Basal ganglia
Animal model
Neurophysiology

ABSTRACT

Tourette syndrome (TS) and attention deficit hyperactivity disorder (ADHD) are two neurodevelopmental hyper-behavioral disorders that are highly comorbid. The source of this comorbidity and the neuronal mechanisms underlying these disorders are still unclear. We examined the neuronal activity of freely behaving rats before and after striatal disinhibition, to reveal the similar and distinct neuronal components underlying the mechanisms of TS-like and ADHD-like symptom expression. Focal disinhibition induced motor tics, locomotor hyperactivity or a comorbid effect depending on the location of the injection within the different functional domains of the striatum. While injections within the motor domain induced motor tics, injections into the limbic domain induced mainly locomotor hyperactivity. Disinhibition, regardless of its striatal location, led to qualitatively similar macro-scale and micro-scale neuronal changes. These changes were localized to the domain of the manipulation and remained partly segregated, indicating that hyperactivity is induced as a result of changes in the limbic domain without directly activating the motor domain. Despite the general similarity of induced neuronal changes, these changes were associated with different behavioral effects and were more stereotypic and pronounced following motor-domain disinhibition in comparison to limbic-domain disinhibition. Our recordings revealed a disparity in the neuronal input–output transformation of the two models of the disorders. The results suggest that tic expression and hyperactivity states share similar local neuronal activity changes which manifest in different neuronal and behavioral outcomes. These results expose an intriguing link between tics and their comorbid symptoms and hint at striatal disinhibition, resulting from GABAergic alterations, as a potential common mechanism underlying distinct symptoms expressed by hyper-behavioral patients.

Abbreviations: ADHD, Attention Deficit Hyperactivity Disorder; BG, Basal Ganglia; CBG, Cortico-Basal Ganglia; FSI, Fast Spiking Interneuron; ILI, Inter LFP-spike Interval; LFP, Local Field Potential; MUA, Multi-Unit Activity; NAc, Nucleus Accumbens; SPN, Spiny Projection Neuron; SU-ST, Single-Unit Spike Train; TS, Tourette Syndrome.

* *Corresponding author*. Bar-Ilan University, Gonda Brain Research Center, Ramat-Gan 52900, Israel.
E-mail address: izhar.bar-gad@biu.ac.il (I. Bar-Gad).

https://doi.org/10.1016/j.cortex.2020.02.010
0010-9452/

1. Introduction

The term *hyper-behavioral disorder* is a blanket term encompassing a wide variety of disorders characterized by an increase in normal and/or abnormal behaviors. One subset of closely related hyper-behavioral disorders includes Tourette syndrome (TS), and attention deficit hyperactivity disorder (ADHD). These disorders are neurodevelopmental and highly comorbid, as most TS patients (>50%) also contend with ADHD (Freeman et al., 2000; Schlaggar & Mink, 2016). In each disorder, the hyper-behavioral condition is manifested differently. TS is characterized by the expression of tics; i.e., rapid and repetitive vocalizations and movements (American Psychiatric Association, 2013) whereas ADHD is characterized by attention difficulties, hyperactivity and impulsivity (Giedd, Blumenthal, Molloy, & Castellanos, 2006; Qiu et al., 2009).

The factors determining the comorbidity of TS and ADHD are unclear and the underlying neuronal mechanism of each disorder is still vague. However, both disorders have been linked to abnormal neuronal activity in the basal ganglia (BG) in general, and the main input nucleus of the BG – the striatum, in particular. The striatum contains feedforward and feedback GABAergic connections encompassing projection neurons as well as interneurons composing a vast inhibitory network (Koós & Tepper, 1999; Tunstall, Oorschot, Kean, & Wickens, 2002). Information flows through the cortico-BG (CBG) loop in three main functional circuits – including the motor, limbic and associative territories (Alexander, DeLong, & Strick, 1986). These functional loops are thought to be mainly parallel as this structure is maintained by the predominantly anatomical separation of the projections throughout all stages of the CBG loop (Alexander et al., 1986; Parent & Hazrati, 1995), although some information flow exists between these domains (Draganski et al., 2008; Haber, 2003). In the striatum, the dorsolateral regions are associated with the motor territory, the dorsomedial regions are associated with the executive/associative territory and the ventral regions, including the nucleus accumbens (NAc), are associated with the limbic territory (Cospito & Kultas-Ilinsky, 1981; Heilbronner, Rodriguez-Romaguera, Quirk, Groenewegen, & Haber, 2016; McGeorge & Faull, 1989). The dorsolateral striatum receives excitatory glutamatergic afferents mainly from 'motor' structures, such as the supplementary motor area and the motor, premotor, and somatosensory cortex (Kunzle, 1975, 1977, 1978), and project mainly to the dorsal region of the globus pallidus and substantia nigra (Szabo, 1967). The NAc receives input primarily from 'limbic' structures, such as the prefrontal cortex, ventral hippocampus and basolateral amygdala (Friedman, Aggleton, & Saunders, 2002; Phillipson & Griffiths, 1985), and send efferents mainly to the ventral pallidum and the ventral region of the substantia nigra (Szabo, 1967). The NAc is further divided into a core and a shell, each of which has unique anatomical and functional features (Heimer, Zahm, Churchill, Kalivas, & Wohltmann, 1991; Voorn, Gerfen, & Groenewegen, 1989). The core and shell differ in their connectivity with other brain regions, making the NAc core part of the ventral striatum, and the NAc shell part of the extended amygdala (Heimer et al., 1997). As part of the limbic territory, the NAc has been found to play a role in reward (Al-Hasani et al., 2015; Berns, McClure, Pagnoni, & Montague, 2001; Floresco, Montes, Tse, & van Holstein, 2018; Robbins, Cador, Taylor, & Everitt, 1989), risk-taking behaviors (Kuhnen & Knutson, 2005), impulsivity (Basar et al., 2010) and feeding behavior (Kelley, Baldo, Pratt, & Will, 2005). Nevertheless, despite the limbic functions currently attributed to the NAc, earlier works suggested that the NAc might play a possible role in controlling overall activity in general, and locomotion in particular (Mogenson & Nielsen, 1984). This raises the hypothesis that the NAc serves as a functional interface between the limbic and motor systems (Mogenson, Jones, & Yim, 1980).

Multiple studies of human TS and ADHD patients point to the prominent role of the CBG loop in their pathophysiology (Giedd et al., 2006). Neuroimaging studies have found altered activations in the BG of these patients (Durston et al., 2003; Peterson et al., 1998; Mink, 2001). Anatomical studies have found a reduction in the overall striatal volume in both disorders (Bloch, Leckman, Zhu, & Peterson, 2005; Carmona et al., 2009; Greven et al., 2015; Kalanithi et al., 2005; Kataoka et al., 2010; Peterson et al., 2003; Qiu et al., 2009). In ADHD this reduction has been found in particular in the ventral striatum (Carmona et al., 2009; Qiu et al., 2009), while in TS it is mainly located in the caudate nucleus (Bloch et al., 2005; Peterson et al., 2003) and expressed by a substantial reduction in the cell count of fast spiking interneurons (FSIs) and tonically active neurons (TANs) (Kalanithi et al., 2005; Kataoka et al., 2010). Further support for the relationship between TS and ADHD to the BG, arises from animal studies. Hyperactivity can be produced by pharmacologically increasing the activity of the NAc core using glutamatergic (Arnt, 1981; Swanson & Kalivas, 2000; Wu, Brudzynski, & Mogenson, 1993), cholinergic (Austin & Kalivas, 1988) and dopaminergic (Costall, Domeney, & Naylor, 1984; Costall & Naylor, 1975a, 1975b; Jones, Mogenson, & Wu, 1981) agonists. Studies inducing focal disinhibition in different functional regions within the striatum (by blocking $GABA_A$ transmission) have produced variety of hyper-behavioral symptoms such as motor and vocal tics as well as hyperactivity and stereotypies in primates and rodents. The induced symptoms were region specific: Focal disinhibition within the limbic striatum or the border between the associative and limbic territories within the striatum, produced hyperactivity, stereotypy (Worbe et al., 2009, 2013) and vocal tics (McCairn et al., 2016) in non-human primates, and increased locomotion in cats and rats (Morgenstern, Mende, Gold, Lemme, & Oelssner, 1984; Wong, Eshel, Dreher, Ong, & Jackson, 1991; Yael, Tahary, Gurovich, Belelovsky, & Bar-Gad, 2019; Yoshida, Nagatsuka, Muramatsu, & Niijima, 1991). Similar focal disinhibition within the dorsolateral striatum was shown to induce motor tics in non-human primates, rats and mice (Bronfeld, Yael, Belelovsky, & Bar-Gad, 2013; McCairn, Bronfeld, Belelovsky, & Bar-Gad, 2009; Pogorelov, Xu, Smith, Buchanan, & Pittenger, 2015; Tarsy, Pycock, Meldrum, & Marsden, 1978; Worbe et al., 2009). The body region expressing the tics was defined by the location of the injection within the dorsolateral

striatum (Bronfeld, Yael, et al., 2013) following the somatotopic organization of the motor territory (Alexander & DeLong, 1985; Brown, Smith, & Goldbloom, 1998). The striatum comprises a thicket of GABAergic connections, containing both feedforward and feedback collaterals via interneurons (primarily FSIs) and medium spiny projection neurons (SPNs), respectively (Bennett & Bolam, 1994; Koós & Tepper, 1999) as well as feedback from the GP (Mallet et al., 2012). It is assumed that the GABAergic manipulation alters these connections unselectively.

These studies suggest that similar neuronal changes may be associated with motor tics and their common comorbidities. However, the neuronal mechanism underlying this comorbidity is still unclear. Previous works employing simultaneous tracking of behavior and neuronal activity from animal models of motor tics and hyperactivity have identified related electrophysiological features (Israelashvili & Bar-Gad, 2015; Vinner, Israelashvili, & Bar-Gad, 2017; Yael et al., 2019). Here we present a novel analysis of an expanded dataset and integrate key concepts derived from data acquired in these experiments, in order to shed light on the similar and distinct neuronal components underlying TS and ADHD.

2. Materials and methods

2.1. Animals

38 female adult Long–Evans rats weighing 279.6 ± 29 g (Mean ± SD) were used in this study. The animals were divided into 3 groups as follows: 20 Ventral acute injection animals [5 previously undescribed animals in addition to all (15) animals described in (Yael et al., 2019)]. 11 Dorsal acute injection animals [2 previously undescribed animals in addition to 9 animals that were described in (Israelashvili & Bar-Gad, 2015)]. 7 Dorsal chronic injection animals [1 previously undescribed animal in addition to all (6) animals described in (Vinner et al., 2017)]. New animals were included in this research in order to add two novel datasets: 1) 9-axis kinematic monitoring for dorsal injections. 2) Simultaneous neuronal recordings form the same functional loop as the injection, as well as from a different functional loop than the injection site. The rats were caged in pairs in IVC system racks and maintained under controlled temperature, a 12 h light/dark cycle and had free access to food and water. All procedures were approved and supervised by the Institutional Animal Care and Use Committee and were in accordance with the National Institutes of Health Guide for the Care and Use of Laboratory Animals and the Bar-Ilan University Guidelines for the Use and Care of Laboratory Animals in Research. This study was approved by the National Committee for Experiments in Laboratory Animals at the Ministry of Health.

2.2. Surgery

The animals underwent surgical procedures for unilateral implantation of an injection cannula and one or more recording arrays. All the surgical procedures and experimental designs have been described in detail in previous manuscripts from our lab (Israelashvili & Bar-Gad, 2015; Vinner et al., 2017; Yael et al., 2019). Briefly, an injection cannula was implanted in an AP angle of 15° or 26° (for acute ventral/anterior striatal injections, respectively), targeting either the NAc core (injection target: AP, 1.5 mm; ML, 2.2 mm; DV, 7 mm; 20 animals) or the anterior striatum (injection target: AP, 1.4 mm; ML, 2.5 mm; DV, 4.6 mm; 9 animals & AP, 1 mm; ML, 2.5 mm; DV, 5 mm; 9 animals). In 7 of the anterior striatum animals, the cannula was connected to a mini-osmotic pump implanted subcutaneously in the back of the rat to enable chronic, continuous infusion (Vinner et al., 2017). Custom-made movable bundles of 32 or 16 Formvar isolated nichrome microwires (impedance ~300 kΩ; 25 μm diameter, A-M systems; Yael et al., 2013) were implanted in the ventromedial striatum (AP, 0.5 mm; ML, 2.2 mm; DV, 5–7 mm; 20 animals), or the dorsolateral striatum (AP, 0.25 mm; ML, 3.75 mm; DV, 4–6 mm; 9 animals, and 1 mm medial in 9 animals). In four animals with ventromedial implantation, an additional recording array was implanted in the dorsolateral striatum (AP, 0.5 mm; ML, 4.0 mm; DV, 3.5–5.5 mm).

2.3. Experimental sessions

The experiments began following a recovery period of at least a week after the operation. Bicuculline methiodide (Sigma–Aldrich) was dissolved in artificial CSF to a final concentration of 1 μg/μl. Microinjections of bicuculline (a median volume of 0.35 μl in anterior injections, and 0.5 μl in ventral injections) were pressure injected through an injection cannula at a rate of 0.35 or 0.5 μl/min, respectively. Previously, it has been shown that anterior injections using a volume of 0.5 μl, result in qualitatively similar effects as those resulting from a volume of 0.35 μl (Bronfeld, Yael, et al., 2013). In the 7 chronic (micro-pump implanter) animals, the total injected bicuculline volume was 200 μl, released over a period of 7 days at a release rate of 1 μl/h. Previous studies demonstrated that comparable bicuculline injection spreads in an ellipsoid with an approximate diameter of <1 mm around the injection site (Yoshida et al., 1991). In 23/55 ventral injection sessions, the injections were performed in DV 8 mm (1 mm below the cannula target) using an extended injection cannula.

During the experimental sessions, the neuronal data were recorded continuously while the animals were awake and moving freely in the recording arena. The neurophysiological data were obtained using 16/32 channels of either wired or wireless acquisition systems. In the wired system, the signal was amplified (X200), band-pass filtered (0.5–10000 Hz, four-pole Butterworth filter), and continuously sampled at 44 kHz. In the wireless system, the signal was amplified (X200), band-pass filtered [1–7000 (16Ch) or 10,000 (32Ch) Hz, one-pole (16Ch) or three-pole (32Ch) Butterworth filter] and continuously sampled at 29.297 (16Ch) or 32 (32Ch) kHz.

During all the recording sessions, the animals' behavior was monitored using at least one 50/60 frames/s video

camera. In experiments using the wireless acquisition system, the behavior was also monitored using 9-axis kinematic (3D accelerometers, gyroscopes and magnetometers) sensors located above the skull within the wireless system.

2.4. Data pre-processing

As described in detail elsewhere (Israelashvili & Bar-Gad, 2015; Moran & Bar-Gad, 2010; Yael et al., 2019), the recorded data were pre-processed offline to extract the local field potential (LFP), the multi-unit activity (MUA) and the single-unit spike trains (SU-ST). Briefly, the LFP signal was extracted using low-pass filtering (40 Hz, four-pole Butterworth filter). Detection of LFP spikes was obtained using an adaptive threshold-crossing method. The threshold was set for each session individually based on the Signal-to-Noise ratio (SNR) (>2). Noisy periods (low SNR) were removed from further analyses. The high frequency part of the signal was extracted from the raw signal using band-pass filtering (300–6000 Hz, four -pole Butterworth filter) and used to study both MUA and SU-ST. The MUA was obtained from the high frequency signal by low-pass filtering (30 Hz, four-pole Butterworth filter) the absolute values (full wave rectification) of the signal to get its envelope. The high frequency signal was additionally sorted into multiple SU-STs using an offline sorter (Plexon). The SU-ST of stable neurons identified as SPNs or FSIs based on their waveform shape and duration, firing rate and firing pattern, were used for further analyses. Auto- and cross-correlation functions were used to identify individual neurons (Harris, Henze, Csicsvari, Hirase, & Buzsaki, 2000): Neurons were included in this study if they had a clear refractory period in the auto-correlation function (rejecting the possibility of a multi-unit), and no refractory period in the cross-correlation function (rejecting the same neuron across multiple clusters). All additional analyses were performed using custom-written MATLAB code (V2014B; MathWorks).

The animals' location and velocity calculations were performed using offline frame-by-frame video analyses to extract the 2- dimensional location of the rats (Yael et al., 2019). A threshold-crossing method was applied to the velocity signal to detect terminations in the animals' locomotion [for more information, see (Yael et al., 2019)].

2.5. Data analysis

We report how we determined our sample size, all data exclusions, all inclusion/exclusion criteria, whether inclusion/exclusion criteria were established prior to data analysis, all manipulations, and all measures in the study. No part of the study procedures or analyses was pre-registered prior to the research being conducted.

All study data and code that necessary to reproduce all analyses and data presentations are available at: https://data.mendeley.com/datasets/k872jmjtgv/draft?a=2752fb08-c21d-4149-b6db-e8fd2d03a8c3.

The correlations between neuronal activity and unitary events such as motor tics, and LFP spikes, was assessed through peri-event time histograms (PETH), using the individual event (tics/LFP spikes) times as a point process. The PETH was calculated using 1 msec bins and was smoothed with a Gaussian window (SD of 10 msec). Significant event-related neuronal activity was determined by calculating the two-tailed confidence intervals based on the PETH tail distribution (2 sec–0.1 sec prior to event time) with a Bonferroni correction for multiple comparisons. Notably, neurons with a very low firing rate (such as SPN neurons) can suffer from a floor effect, since inhibitions may not be detected, leading to an underestimate of these responses. In order to quantify the percentage of LFP spikes in each session to which an individual significantly-correlated neuron showed altered neuronal activity, we compared the number of spikes for each neuron around each LFP spike to the median number of spikes that this neuron fired at 1000 random time windows of 100 msec in between LFP spikes (between 1 sec and 0.1 sec prior LFP spike times). This percentage was calculated separately for the first phase (100 msec post LFP spike initiation time), and the second phase (100–200 msec post LFP spike time).

Overall firing rate changes were assessed by comparing the baseline firing rate of neurons pre- and post-bicuculline injection (pre: 26.8 ± 6.8, post: 21.6 ± 11.1 min; mean ± SD) using a Wilcoxon rank sum test. The mean firing rate of the population was calculated using all the neurons that were recorded throughout the normal and/or tic/hyperactivity periods. Since some neurons were only recorded following injections, and other neurons only prior to the injections, the two groups are not matched. Overall firing rate changes around LFP spikes were assessed by comparing the baseline firing rate of each neuron prior the LFP spikes (calculated over the 0.5 to 0.1 sec interval prior to LFP spike onsets) to the baseline firing rate at two periods during LFP spike occurrence times (0–0.1 sec following LFP spike onset, and 0.1–0.2 sec following LFP spike onset) using a Wilcoxon signed rank test between each pair of groups. These groups contained neurons that were recorded simultaneously with LFP spikes, and thus did not necessarily contain the same neurons as in the post-injection group (used for the baseline firing rate calculation).

Cross-correlations between simultaneously recorded pairs of neurons were calculated using a time resolution of 1 msec bins and smoothed using a Gaussian window (SD of 2 msec). Different neurons recorded on the same electrode were excluded from the cross correlation analysis to avoid artificial correlations (Bar-Gad, Ritov, Vaadia, & Bergman, 2001).

Part of the dataset used in the manuscript was presented in previous studies (Israelashvili & Bar-Gad, 2015; Vinner, Israelashvili, & Bar-Gad, 2017; Yael, Tahary, Gurovich, Belelovsky, & Bar-Gad, 2019). Here, besides performing a controlled comparison between the neuronal mechanisms of tics and hyperactivity as well as expanding the number of animals and experiments for each of the behavioral states (see Materials and Methods – 2.1 Animals), we added several novel neuronal activity types and analyses: examination of the multi-unit activity, comparison between the neuronal activities that were recorded from two different functional territories simultaneously, extended quantification of the characteristic of macro- and micro-neuronal changes in both behavioral states and completion of new data and analyses

that were currently missing from previous studies of the two behavioral states.

2.6. Histology

At the end of the experimental sessions, the rats were deeply anesthetized, the location of the electrode tips and microinjections were marked and the rats were transcardially perfused in order to extract their brain (Israelashvili & Bar-Gad, 2015; Yael et al., 2019). Coronal sections (50 μm) were used to examine and verify the implanted structures. Examples of histological reconstruction are shown in Vinner et al., 2017; Yael et al., 2019.

3. Results

3.1. Striatal bicuculline injections lead to location-dependent symptoms

Bicuculline ($GABA_A$ antagonist) was injected into either the dorsal (motor) or the ventral (limbic) regions of the rats' striatum inducing motor tics and/or hyperactivity (Movie 1), depending on the injection site within the striatum. All the injections into the dorsal part of the striatum (n = 41 injections in 18 rats) induced motor tics (Fig. 1). In contrast, injections in the ventral parts of the striatum (n = 55 injections in 20 rats) induced hyperactivity in most cases, but in some cases resulted in a comorbid effect of motor tics with hyperactivity, or even only motor tics (Fig. 1). The animals' behavior was tracked before and after the injections, using high-speed video recordings and 3D motion sensors (accelerometers and gyroscopes). Tics were characterized as focal, repetitive, brief muscle contractions, whereas hyperactivity was expressed as increased locomotion as well as increased normal behavior (Fig. 2) [for more details see (Bronfeld, Yael, et al., 2013; Israelashvili & Bar-Gad, 2015; Vinner et al., 2017; Yael et al., 2019)]. For clarity reasons, we will refer to dorsal/ventral injections as tic/hyperactivity states (respectively), instead of using the explicit anatomical terms.

Supplementary video related to this article can be found at https://doi.org/10.1016/j.cortex.2020.02.010

3.2. Diverse neuronal signals

Neuronal recordings from sessions with pure motor tics or pure hyperactivity were further analyzed. The recordings were performed using electrodes implanted in the dorsal and/or the ventral parts of the striatum near the injection site. A set of neuronal signals were examined and extracted from the raw neurophysiological data as follows. 1) The local field potential (LFP) signal is a summation of slowly alternating electrical currents originating from a large neuronal volume (radius ~ 0.5–3.0 mm depending on multiple factors, primarily the neuronal organization in the tissue) located around the electrode tip (Juergens, Guettler, & Eckhorn, 1999; Mitzdorf, 1987). It represents the low frequency changes in the signal which are assumed to primarily reflect the synaptic inputs to the recorded site [but see (Logothetis, 2003) for additional sources of the signal]. The LFP was obtained from the recorded data using a low-pass filter (frequencies <40 Hz) (Fig. 3A and B). The high frequency (>300 Hz) part of the signal was used to study the activity of both multi-unit activity (MUA) and single unit spike trains (SU-ST). 2) MUA represents the summation of the spiking activity from multiple nearby neurons (radius ~ 200–300 μm, depending on the size and shape of the neurons and the electrode's properties) (Lemon, 1984; Logothetis, 2002). The MUA signal was obtained by extracting the low frequency envelope of the high frequency signal (Fig. 3A and B). 3) SU-ST refers to the spiking times (discrete events) of individual neurons around the tip of the electrode (radius <50 μm) (Henze et al., 2000; Lemon, 1984) (Fig. 3A and B). SU-STs were obtained from the high frequency signal using offline sorting to one or more SU-STs. These three signals reflect different neural components and thus provide different information regarding essential neuronal principles underlying hyper-behavioral states. For example, by aligning these signals to time points of interest in the data such as motor tics, different types of neuronal changes can be observed. These changes may comprise macro-scale as well as micro-scale neuronal changes, depending on the scale of the neural population they represent. Thus, macro-scale changes can be detected by exploring the LFP signal, and micro-scale neuronal changes at different scales can be revealed by examining the MUA and the SU-ST (Fig. 3C).

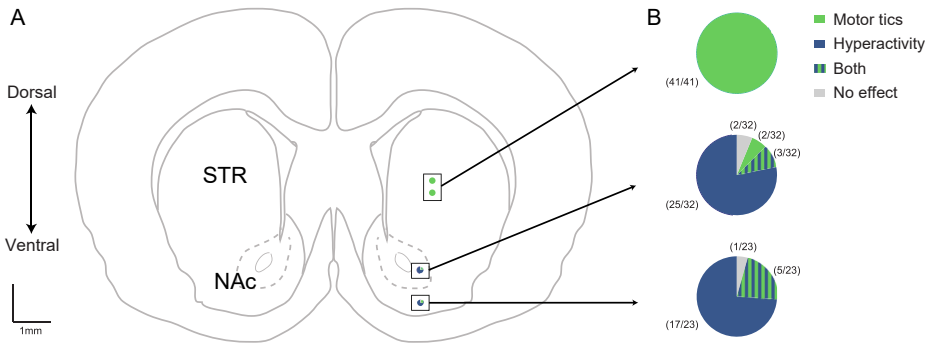

Fig. 1 – Behavioral effects of striatal disinhibition. (A) Schematic illustration of the injection locations and the induced behavior over a coronal section of the rat brain. (B) Zoom in on the distributions of the induced behavioral effects at each depth.

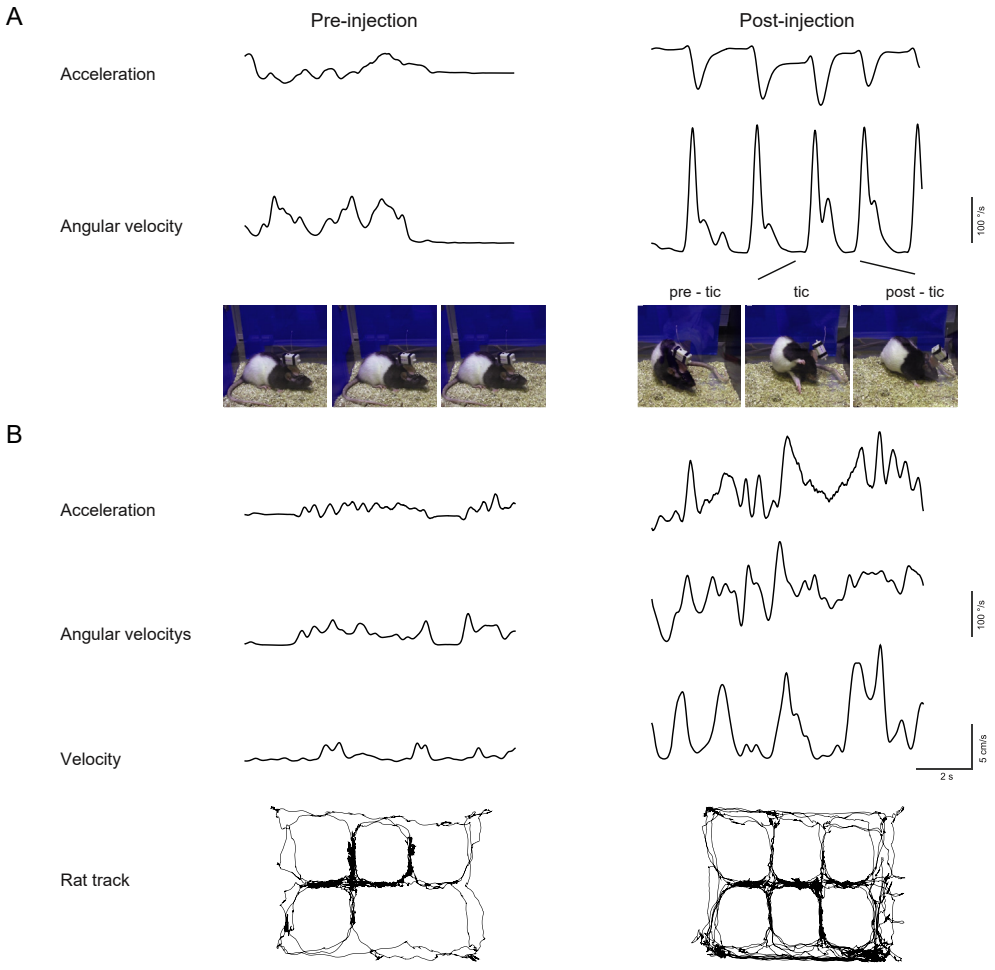

Fig. 2 – Behavioral characteristics of the induced hyper-behavior. An example of (A) tic expression and (B) increased locomotion subsequent to a bicuculline injection to the dorsal and ventral striatum, respectively.

3.3. *Macro neuronal changes*

In both hyper-behavioral states (motor tics and hyperactivity) low-frequency changes were observed in the LFP signal. These changes were termed *LFP spikes* and were not apparent during the animals' normal state prior to the injections (Fig. 4 A). The rate of these macro neuronal changes exhibited similar properties in the two hyper-behavioral states. In both states, the inter LFP spike intervals (ILIs) were exponentially distributed, suggesting that the LFP spikes followed a Poisson distribution (Fig. 4 B). In both states, the distributions were truncated at the short interval values indicative of a refractory period of the LFP spikes, which is in line with studies using cortical stimulation to force the expression of tics (Israelashvili & Bar-Gad, 2015). For each session (single injection in a single animal), the LFP spike refractory period was defined as the minimal inter-LFP spike interval across all LFP spikes in this session. The refractory periods were shorter during the hyperactivity state than during tic expression (two-sample t-test $t = 3.48$, $df = 26$, $p < 0.01$); specifically, the shortest ILI across all experiments was 0.28 sec following dorsal injections, and 0.22 sec following ventral injections. The frequency of the LFP spikes varied across animals, but in general was higher following dorsal injections (dorsal: 0.51 ± 0.24 Hz, ventral: 0.33 ± 0.15 Hz, mean ± SD, two-sample t-test $t = 2.18$, $df = 26$, $p < 0.05$) (Fig. 4C). The LFP spike shapes were highly stereotypic in shape within each experimental session, but varied across sessions (Vinner et al., 2017), especially following dorsal injections (Fig. 4 D). This variation may result from differences in the relative distance/location between the recording electrode and the injection site (Muramatsu, Yoshida, & Nakamura, 1990). In general, regardless of the variation in shapes, the first phase in the LFP spike shape, from initiation time to the first zero crossing (20–200 msec) of the mean shape, was wider during hyperactivity than during motor tics (dorsal: 93 ± 8 msec, ventral: 167 ± 6 msec, mean ± SEM, two-sample t-test $t = -6.2$, $df = 49$, $p < 0.01$). In some (8/18) of the experiments used for macro change analyses following ventral injections, we recorded neuronal activity simultaneously from both the ventral and dorsal regions within the striatum. After the ventral injections, LFP spikes were also observed in the dorsal regions of the striatum (Fig. 4 E). These LFP spikes were similar in shape (0.89 ± 0.04, mean ± SEM, Pearson's product–moment correlation coefficient), but smaller in amplitude (Wilcoxon signed rank test, $p < 0.01$)

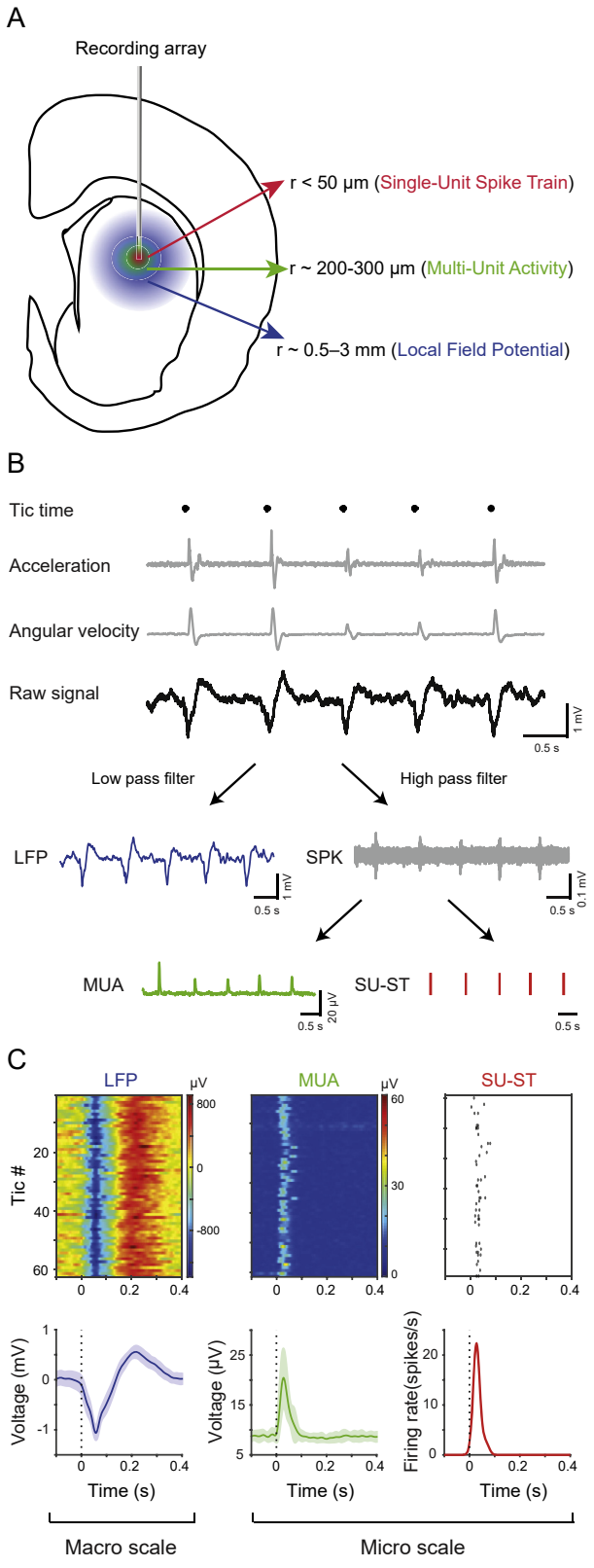

Fig. 3 – Types of neuronal signals. (A) Schematic illustration of the neuronal volume affecting each type of neuronal signal. (B) Example of the different signals and their extraction from the recorded raw data. (C) Peri-tic signal (top) and the mean shape (or histogram) (bold) ± one SD (shaded) (bottom). Black dotted lines indicate the tic times.

than their corresponding LFP spikes in the ventral striatum (Fig. 4F and G). In addition, the ventral LFP spikes mostly preceded the dorsal LFP spikes (7 msec, median, Wilcoxon signed rank test, $p < 0.01$). Thus suggesting that the LFP spikes from the ventral injection spread from the ventral striatum to its dorsal part.

3.4. *Micro neuronal changes*

Changes in the activity of individual neurons were analyzed in both hyper-behavioral states. We recorded the activity of 84 spiny projection neurons (SPNs - 41 dorsal, 43 ventral) and 38 fast spiking inter-neurons (FSIs - 29 dorsal, 9 ventral) simultaneously with LFP spike recordings. In both states, the neurons exhibited altered neuronal activity around the time of LFP spikes (Fig. 5 A). 92.7% (38/41) of the recorded SPNs displayed significant LFP spike-related activity during the motor tic state, and 74.4% (32/43) of the recorded SPNs displayed significant LFP spike-related activity during the hyperactivity state (Fig. 5 B). During tics, all the significantly locked SPNs showed a phase of increase in their firing rate around the time of the LFP spikes (Fig. 5 B). During hyperactivity, most locked SPNs (28/32) displayed a phase of decrease in their activity. This decrease was preceded by a short increase in firing rate in some of the neurons (12/28). Most of the recorded FSIs in both states [86.2% (25/29) during the motor tic state, and 100% (9/9) during the hyperactivity state], displayed significant LFP spike-related activity. During tics, most of the significantly modulated FSIs (21/25) displayed an increase in activity around the LFP spikes which was followed by a decrease in activity in a minority of these neurons (7/25). However, during the hyperactivity state, most of the FSIs (7/9) had both increased and decreased firing rate phases (Fig. 5 B). The mean response of the SPN as well as the FSI locked population was characterized by short excitation followed by lower amplitude prolonged excitation during tics, or inhibition during hyperactivity (Fig. 5C). The overall baseline firing rate increased after injection only in the dorsal SPN neurons (Wilcoxon rank sum test, $p < 0.01$) (Fig. 5 D). Around the LFP spikes the mean firing rate increased during tics (from 0 to 100 msec post LFP spike window) and decreased during hyperactivity (from 100 to 200 msec post LFP spike window), for both neuronal populations (Wilcoxon signed rank test) (Fig. 5 E).

3.5. *Behavior-related neuronal changes*

Injections in the motor and limbic regions of the striatum led to macro-scale as well as micro-scale neuronal changes throughout the striatum. However, despite sharing qualitatively similar types of neuronal changes (macro- and micro-neuronal changes) and a similar causal factor (focal disinhibition), the injections induced very different behaviors. We examined the relationship between the macro and micro neuronal changes to each type of behavior. On the macro scale, LFP spikes were associated with behavioral events in both states. During the motor tic state, all the LFP spikes were associated with the expression of individual tics (Fig. 6 A). This association was injective, since the LFP spikes were observed simultaneously with tics, and did not occur between tics (Fig. 6 B). In the hyperactivity state, LFP spikes were associated

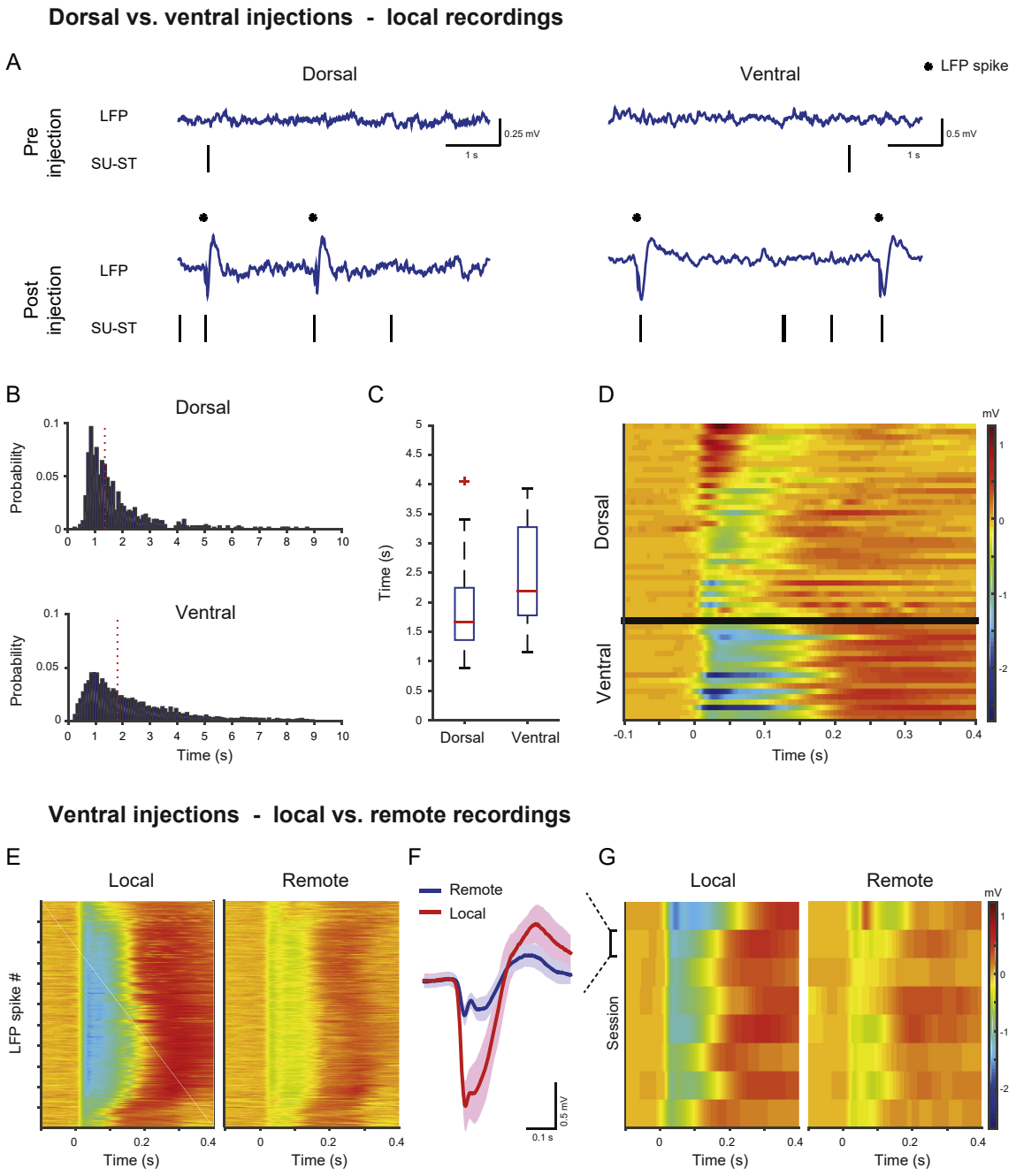

Fig. 4 – Macro-scale neuronal changes. (A–D) Comparison of local neuronal responses to dorsal and ventral injections (A) Example of a LFP signal and SPN SU-STs. (B) Inter LFP-spike interval (ILI) histogram across all sessions. Dotted line – ILI median. (C) Box-plot diagram of the ILI medians per session distribution. (D) Mean LFP spike shapes per session (sorted by the positive phase time). (E–G) Comparison of local and remote neuronal responses to ventral injections. (E) An example of peri-LFP spikes LFP, recorded simultaneously during one session, from the ventral (left) and dorsal (right) striatum, after ventral injection. (F) The mean LFP spike shape (bold) ± one SD (shaded) of the session shown in E. (G) Mean LFP spike shapes per session.

primarily with velocity changes in general, and movement termination in particular (Yael et al., 2019) (Fig. 6 A). However, within each of the related sessions, only a small fraction of the LFP spikes were the cause of this mean change, because the association was sparse and not injective (Fig. 6 B). Similar differences were found on the micro scale: subsequent to the dorsal injections, most neurons displayed altered neuronal activity around a large fraction of the tics (Fig. 6C). After injections to the NAc core, some neurons displayed altered neuronal activity around movement stops (Yael et al., 2019); however, this alteration was weaker and only a smaller fraction of the spikes were associated with velocity changes (Fig. 6C). These results suggest that although both hyper-behavioral states share similar types of neuronal changes

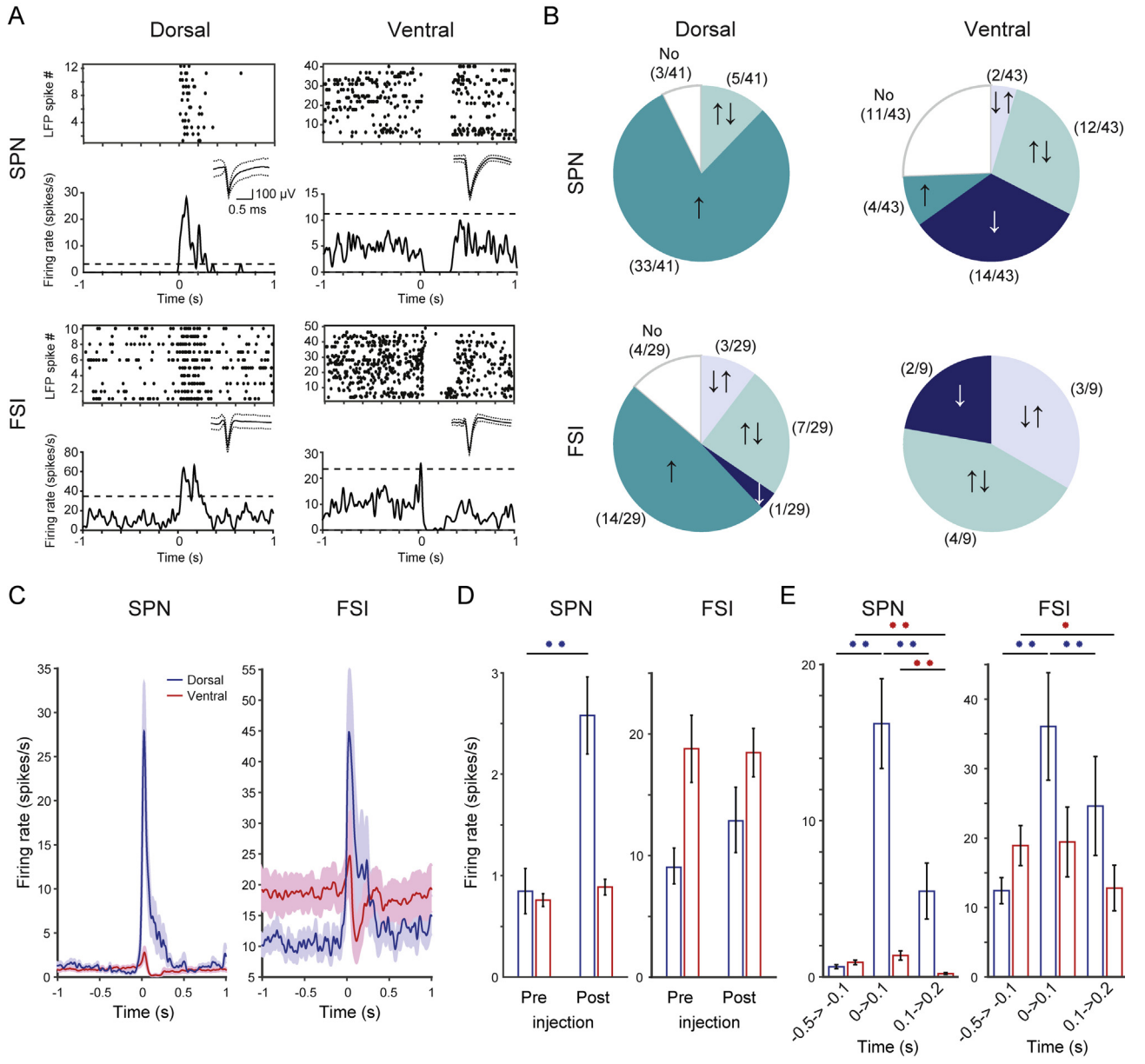

Fig. 5 – Micro-scale neuronal changes. (A) Examples of a peri-LFP spike single neuron raster (top) and histogram (bottom). Black dashed lines mark the 99% confidence intervals. The mean waveform of the individual neurons (solid) ±1 SD (dotted) appears in the inset. (B) Distributions of peri-LFP spike response types. (C) Mean peri-LFP spike response of significantly modulated neurons (bold) ± one SEM (shaded). (D) Mean overall firing rate pre and post injection ± one SEM. **$p < 0.01$. (E) Mean firing rate post injection during different periods around the LFP spikes ± one SEM. *$p < 0.05$, **$p < 0.01$.

(though in different magnitudes), these changes are associated differentially with behavioral events.

3.6. *Synchronized versus sparse encoding*

We compared the population activity and the individual neurons' intrinsic activity around a similar element - the LFP spikes. Differences between the two states were found at the level of multiunit as well as single unit activity around LFP spikes (Fig. 7 A). We examined the MUA subsequent to both injections. In both states, increased multiunit activity was observed around LFP spikes (Fig. 7 Bi). However, these changes in the population activity were prolonged, constant, and much stronger during tics than during hyperactivity (Wilcoxon rank sum test, $p < 0.01$) (Fig. 7 Bii). In 8 recording sessions during the hyperactivity state, we recorded the MUA from both the dorsal and the ventral regions simultaneously. In these experiments, MUA changes were found in both regions. However, on average, these changes manifested as a decrease in MUA and were much weaker in the dorsal portion than in the ventral portion (Wilcoxon rank sum test, $p < 0.05$) (Fig. 7 B) further suggesting that the source of the altered neuronal activity depends on the injection site, and spreads from there throughout the striatum. On the level of SU-ST, even amongst

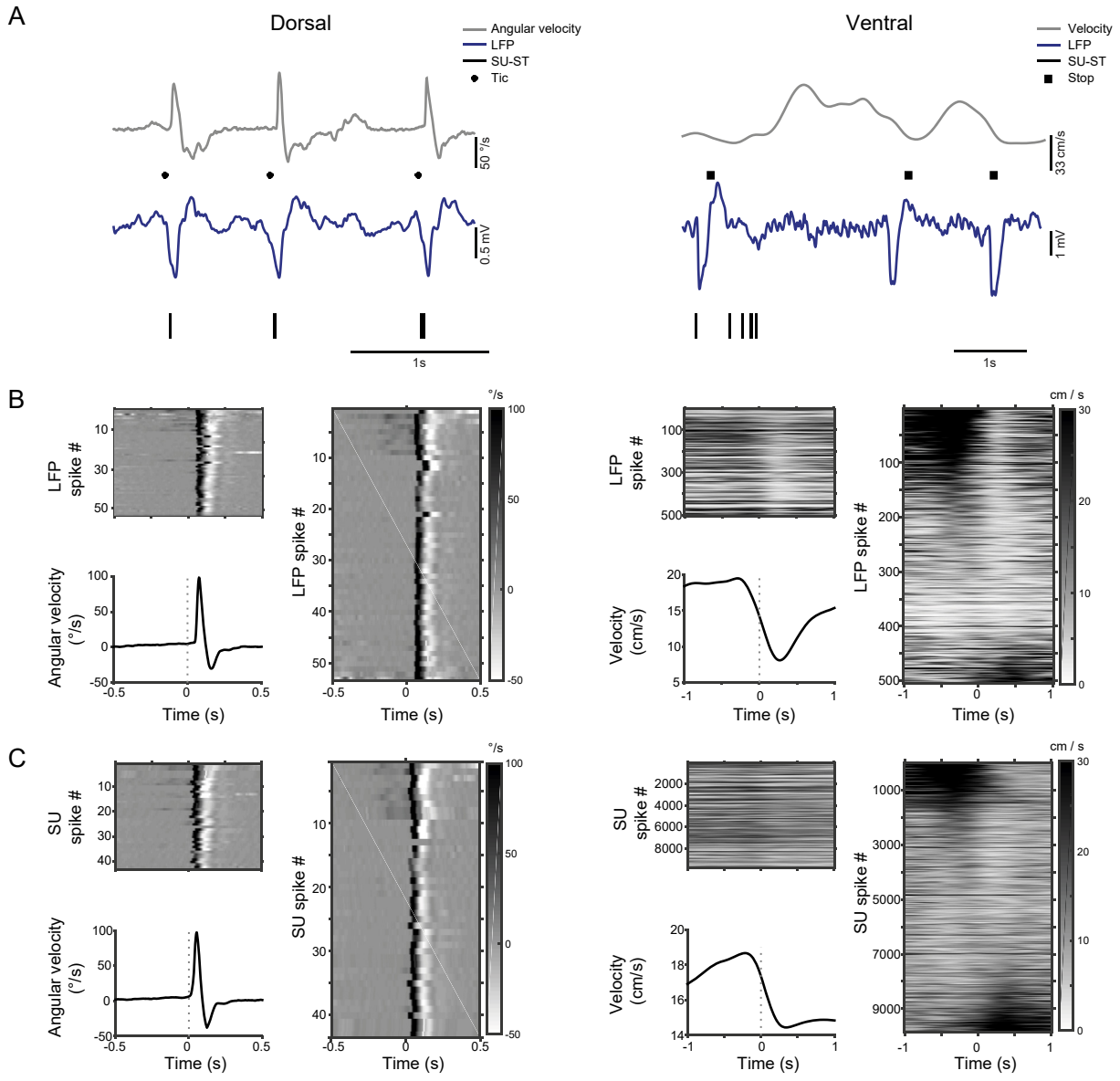

Fig. 6 – Differences in behavior-related neuronal activity changes. (A) An example of the relationship between behavioral events and neuronal macro- and micro-activity. (B) The relationship between LFP spikes and movement. An example taken from a single session (for each state) of (top left) angular velocity (dorsal) and velocity (ventral) around LFP spikes and (bottom left) their mean shape and (right) the same raster sorted as a function of the difference between the mean shape pre-, post- LFP spike onset (±0.5 sec). (C) The relationship between SU-ST and movement. Same as B, but around individual neuron spikes (instead of LFP spikes).

the neurons that were locked to LFP spikes, differences were found within the responses. During tics, neurons were locked to a larger percentage of LFP spikes in each session, unlike the weaker and partially locked response during hyperactivity (Fig. 7C and D). These results point to a stronger net synchronization during tics than during hyperactivity. In order to further examine this assumption, we calculated the correlations between simultaneously recorded SPN neurons in the ventral and dorsal striatum (Fig. 7E and F). Following dorsal striatum disinhibition, neurons showed stronger correlations in comparison to neurons following disinhibition in the NAc core (Wilcoxon rank sum test, $p < 0.01$).

4. Discussion

TS and ADHD are two neurodevelopmental hyper-behavioral disorders that are highly comorbid (Freeman et al., 2000; Schlaggar & Mink, 2016). Here we integrated key concepts from multiple experimental studies to shed light on the similarities and differences between neuronal changes underlying TS and ADHD. Similar focal disinhibition induced different hyper-behavioral symptoms, based on the functional location of the deficit within the striatum. Focal disinhibition in the motor (dorsal) striatum resulted in motor tics whereas focal disinhibition in the limbic (ventral) striatum resulted in

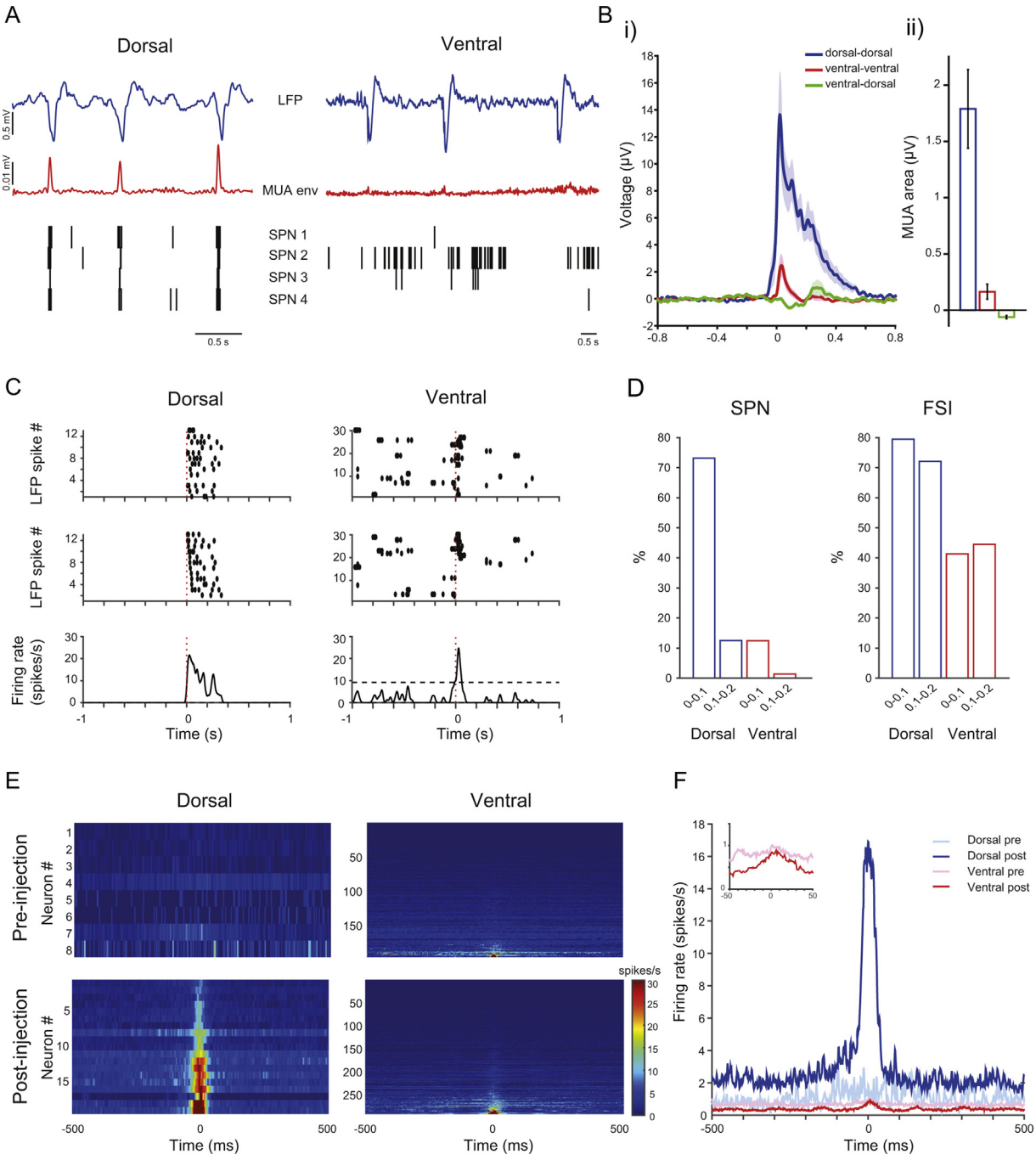

Fig. 7 – Differences in LFP spike related activity. (A) Example of LFP, MUA and SPN SU-STs after the injection. (B) (i) Mean ± SEM (shaded) of the normalized mean MUA shape per session, around the LFP spike times, (ii) and the related mean ± SEM area under the MUA shape curves (trapezoidal numerical integration at ±200 msec around the LFP spike). Blue – dorsal injections, local recordings. Red – ventral injections, local recordings. Green – ventral injections, remote recordings. (C) Example of a peri-LFP spike single neuron raster (top), the same raster sorted as a function of the latency between LFP spikes onset and the neuron spikes (middle) and the histogram (bottom). Dashed black lines mark the 99% confidence intervals. (D) The median percentage of LFP spikes within each session that were related to single neuron spiking modulations. (E) Cross-correlation functions of all the simultaneously recorded SPN single unit pairs. (F) Median cross-correlation functions across all pairs. Zoom in appears in the inset.

prolonged locomotor hyperactivity. These manipulations, regardless of their location within the striatum, led to similar types of macro-scale as well as micro-scale neuronal changes. However, these changes were associated with different behavioral effects and neuronal–behavioral associations. During the tic state, the altered neuronal activity was time-locked to the individual phasic movements (i.e., tics). Whereas, during the hyperactivity state, the altered neuronal

activity was time-related mainly to phasic changes in velocity. These velocity changes can resample direction changes (for example), in contrast to a full stopping in the increased locomotor activity. Despite sharing similar types of neuronal changes, the two behavioral conditions differed in the distributions of these changes. During tics, the abnormal neuronal activity was stereotypic and highly synchronized. By contrast, during hyperactivity, the abnormal activity changes, although similar in nature, were diverse and sparse and less pronounced, in comparison to the corresponding activity changes during tics (Fig. 8).

Over the years, multiple animal models have been developed to address different properties of TS and ADHD. Each of these models has focused on a specific symptom/feature of these disorders. ADHD is characterized mainly by attention difficulties, hyperactivity and impulsivity (Giedd et al., 2006; Qiu et al., 2009), some of which might be complex to evaluate in an animal model. As measures of locomotor hyperactivity have been shown to be a significant diagnostic tool for children as well as adults with ADHD (García, Cortese, Anderson, Di, & Xavier, 2015), many studies have focused on modeling this symptom. Locomotor hyperactivity, has been successfully induced by variety of models manipulating the activity of the NAc (Arnt, 1981; Jones et al., 1981; Morgenstern et al., 1984; Wachtel, Anden, Helmut, & Nils-Erik, 1978). The common denominator behind all NAc models is that they elevate the excitation within the NAc, either directly or indirectly. This excitation is not specific to a certain neurotransmitter, since local injections of glutamatergic (Arnt, 1981; Swanson & Kalivas, 2000; Wu et al., 1993), cholinergic (Austin & Kalivas, 1988) and dopaminergic (Costall & Naylor, 1975a, 1975b; Costall et al., 1984; Jones et al., 1981) agonists, as well as GABAergic antagonists (Morgenstern et al., 1984; Wong et al., 1991) or mixtures of these agents, result in increased locomotion. In contrast, GABA antagonist injections are currently the only pharmacological manipulations that induce the key symptom of TS – motor (Bronfeld, Israelashvili, & Bar-Gad, 2013; Yael, Israelashvili, & Bar-Gad, 2016) and vocal tics (McCairn et al., 2016). This suggests that focal disinhibition stemming from abnormal GABAergic transmission may be the common neuronal mechanism underlying the two disorders. This notion is further supported by other hyper-behavioral symptoms that can be induced by BG GABAergic

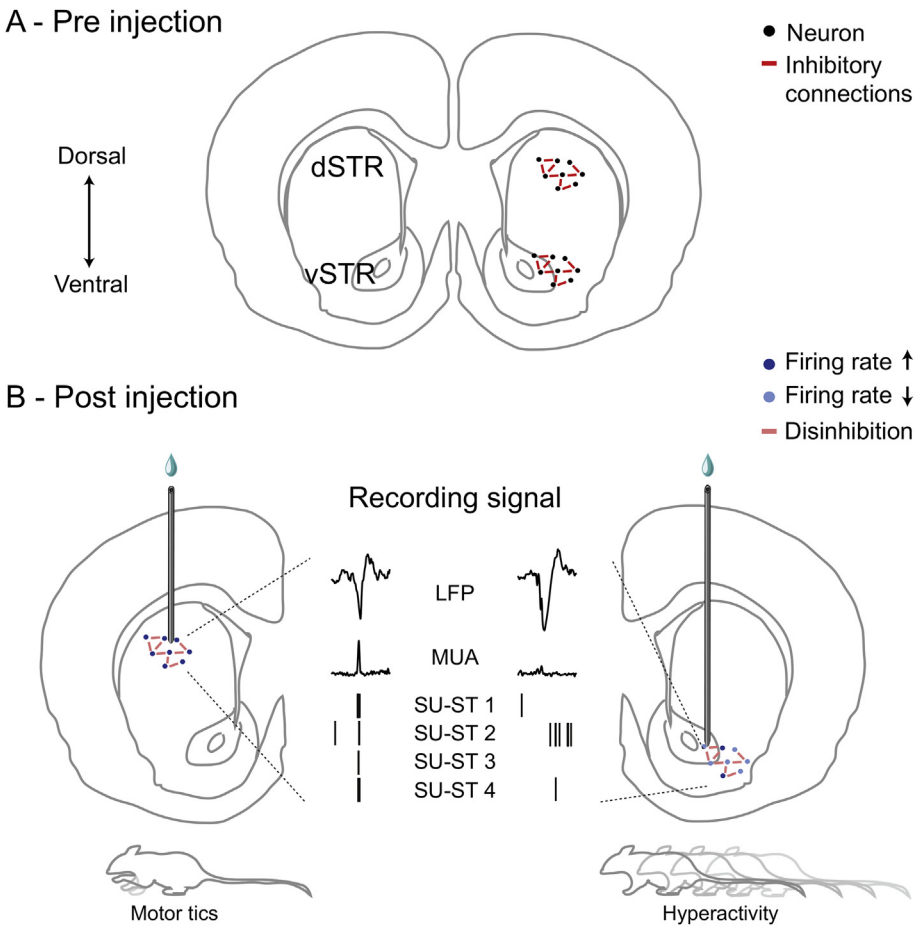

Fig. 8 – Shared neuronal mechanisms underlying tics and hyperactivity. (A) Schematic illustration of a coronal section of the rat brain, detailing the normal inhibitory connections between neurons in the dorsal and ventral regions of the striatum. (B) Schematic illustration of the behavioral and neuronal changes after bicuculline injection into the striatum.

manipulations. Focal microinjection of GABAergic antagonists into different regions within the BG have been shown to result in a variety of hyperkinetic symptoms. Injections into the ventral striatum or the border between the associative and limbic territories within the striatum of non-human primates, induced hyperactivity but also stereotypy (Worbe et al., 2009, 2013) and vocal tics (McCairn et al., 2016). In addition, injections into the globus pallidus externus (GPe) were reported to produce chorea, hyperactivity and stereotypy depending on the functional territory of the injection: motor, associative or limbic, respectively (Bronfeld et al., 2010; Crossman, Mitchell, Sambrook, & Jackson, 1988; François et al., 2004; Grabli et al., 2004; Matsumura, Tremblay, Richard, & Filion, 1995).

In the current study, microinjection of $GABA_A$ antagonist resulted in different hyper-behavior symptoms (motor tics *vs* hyperactivity), depending on the functional location of the injection within the striatum. The induced behaviors were not merely different in terms of type, but also in multiple properties (Table 1). Focal disinhibition in the motor striatum induced abnormal behavior (motor tics) which was phasic in time and space. Specifically, it induced repetitive and rapid abnormal movements that appeared in a specific body region, contralateral to the injected hemisphere. The exact body region of the tics was dependent on the somatotopic location of the injection within the motor striatum (Bronfeld, Yael, et al., 2013). The same injection in the ventral striatum (NAc core) resulted in an increase in normal behavior (locomotion) which was continuous with phasic changes in time and space. Namely, the injection produced a prolonged increase in normal activity of the whole body, regardless of the injection hemisphere (Table 1). This differentiation between normal and abnormal behaviors for characterizing locomotion and motor tics (respectively), is based upon the difference between the occurrence of a complete set of normal behaviors (locomotion) or a subset of them occurring out of context (motor tics). Differences were found also at the neuronal activity level. This behavioral and neuronal divergence between the results of the manipulations clearly underscores the different roles and structures of different functional loops within the BG.

The transformation from focal striatal disinhibition to the induced behavior in the dorsal striatum adheres to the theoretical framework of action selection (Albin & Mink, 2006; Mink, 2001), but this transformation is unclear in the ventral domain. In this study we used neuronal recordings to better unpack this transformation by examining local input–output relations in both domains and their relationship to tics and hyperactivity. In general, strong, synchronized input is expected to induce synchronized focal neuronal activity. This activity may be seen as a strong modulation of MUA as well as in focal input-lock phasic spiking activity which in turn results in focal phasic behavior (such as tics). On the other hand, sparse, weak inputs is not assumed to induce synchronized focal activity, and will result in weak MUA modulation, a sparse input-lock response and a tonic increase in normal behavior. Thus, based on the observed outputs, one would expect to find strong synchronized input in the dorsal region during tics, but sparse and unsynchronized inputs in the ventral region during hyperactivity. Surprisingly, our recordings revealed a neuronal discrepancy between the input–output relations of the two disorders. After injections to either territory, we observed similar macro-scale neuronal alterations ("LFP spikes") which presumably mainly reflect the inputs to the recorded site. Thus, the observation of LFP spikes seems to indicate that in both cases, the local functional striatal domain receives strong synchronized inputs. To preclude the possibility of LFP spread from the dorsal striatum to the ventral striatum being mistakenly considered as arising from ventral origin, we recorded simultaneously in both regions. These recordings revealed weaker, as well as delayed, alterations in the dorsal part relative to the ventral part after ventral injections. This suggests that the source of the altered neuronal activity can be localized to the domain of the injection site, and spreads from there throughout the striatum, thus inducing a cascade of neuronal events that remain partly segregated and result in altered behavior. These data suggest a key difference between the two disorders, since similar synchronized inputs resulted in different outputs: strong, stereotypic modulation and highly synchronized neuronal activity after dorsal injections, but relatively sparse, weak and diverse responses after ventral injection. One possible explanation for the difference in the transformations may have to do with structural differences between the two networks. A possible difference may result from different FSI spatial distributions. FSIs receive direct information from the cortex (Bennett & Bolam, 1994), and feed-forward this information, in the form of inhibition, to SPNs. This inhibition can affect SPN spike timing (Koós & Tepper, 1999). Studies have shown that selective inhibition of FSIs can induce different motor abnormalities (Gittis et al., 2011; Klaus & Plenz, 2016; Oran & Bar-Gad, 2018), indicating that FSIs play a crucial role in equilibrating the activity of the CBG loop. FSIs are not equally distributed across the striatum, but rather are located mainly on the lateral portion of the striatum, potentially affecting primarily the dorsolateral recordings. Alternatively, these differences may be ascribed to the somatotopic distribution within the motor regions of the BG that may facilitate increased synchronization between groups of somatotopically related neurons in the dorsal region (Albin & Mink, 2006; Mink, 2001). Certain discrepancies may have been related to sampling biases in our recordings within the two areas. Earlier studies have shown that there is a core location of locked responses after bicuculline injection into the dorsal striatum (Bronfeld, Belelovsky, & Bar-Gad, 2011; Worbe et al., 2009). We placed the recording electrodes approximately

Table 1 – Behavioral outcomes of dorsal and ventral striatal disinhibition.

Behavior	Functional region	Laterality	Spatial scope	Temporal scope	Movement type
Motor tics	Motor Striatum	Unilateral	Local to body region	Phasic	Abnormal movement
Hyperactivity	Limbic Striatum	Bilateral	Whole body	Continuous with phasic changes	Normal movement

within the same distance from the injection sites in both the dorsal and ventral areas. However, due to differences in micro-architecture we may have recorded outside the core location within the ventral striatum. Potentially recording the surrounding activity, thus leading to the observed higher degree of inhibitory responses compared to excitatory responses of ventral SPNs to LFP spikes.

The observed transformation between neuronal activity and the induced behavior may also be interpreted within the framework of behavioral modification encoding. Our findings showed that LFP spikes were associated with either motor tics or velocity changes (primarily reduction), both of which are types of *action shifts*. The difference in the properties of these shifts is associated with its local functional pathway which encodes either the direct expression of simple movements (tics – dorsal striatum) or the indirect expression of complex movements (velocity changes – ventral striatum). According to this approach the functional pathway determines the overall state and in each state the action shifts are triggered by strong, synchronized cortical inputs in the form of LFP spikes. In line with recent findings (Israelashvili & Bar-Gad, 2015), the striatum appears to determine the type of expressed action based on its organization, whereas input from the corresponding cortical area determines the timing of the discrete action within each continuous state.

5. Conclusion

TS and ADHD are two neurodevelopmental hyper-behavioral disorders that are highly comorbid. Here we showed that tic expression and hyperactivity states share similar local neuronal activity changes which manifest as different neuronal and behavioral outcomes. These results reveal an intriguing link between tics and their comorbid symptoms and point to striatal disinhibition as the common mechanism underlying different symptoms expressed by hyper-behavioral patients.

Funding

This study was supported in part by an Israel Science Foundation (ISF) grant (297/18) and a BSF-NSF Collaborative Research in Computational Neuroscience (CRCNS) grant (2016744).

Open practices

The study in this article earned Open Materials and Open Data badges for transparent practices. Materials and data for the study are available at https://data.mendeley.com/datasets/k872jmjtgv/draft?a=2752fb08-c21d-4149-b6db-e8fd2d03a8c3.

Declaration of Competing Interest

None.

Acknowledgments

We thank D. Olmayev for technical assistance.

REFERENCES

Al-Hasani, R., McCall, J. G., Shin, G., Gomez, A. M., Schmitz, G. P., Bernardi, J. M., et al. (2015). Distinct subpopulations of nucleus accumbens dynorphin neurons drive aversion and reward. *Neuron, 87*(5), 1063–1077.

Albin, R. L., & Mink, J. W. (2006). Recent advances in Tourette syndrome research. *Trends in Neurosciences, 29*(3), 175–182.

Alexander, G. E., & DeLong, M. R. (1985). Microstimulation of the primate neostriatum. II. Somatotopic organization of striatal microexcitable zones and their relation to neuronal response properties. *Journal of Neurophysiology, 53*, 1417–1430.

Alexander, G. E., DeLong, M. R., & Strick, P. L. (1986). Parallel organization of functionally segregated circuits linking basal ganglia and cortex. *Annual Review of Neuroscience, 9*, 357–381.

American Psychiatric Association. (2013). *DSM-5*.

Arnt, J. (1981). Hyperactivity following injection of a glutamate agonist and 6, 7-ADTN into rat nucleus accumbens and its inhibition by THIP. *Life Sciences, 28*(14), 1597–1603.

Austin, M. C., & Kalivas, P. W. (1988). The effect of cholinergic stimulation in the nucleus accumbens on locomotor behavior. *Brain Research, 441*(1–2), 209–214.

Bar-Gad, I., Ritov, Y., Vaadia, E., & Bergman, H. (2001). Failure in identification of overlapping spikes from multiple neuron activity causes artificial correlations. *Journal of Neuroscience Methods, 107*, 1–13.

Basar, K., Sesia, T., Groenewegen, H., Steinbusch, H. W. M., Visser-Vandewalle, V., & Temel, Y. (2010). Nucleus accumbens and impulsivity. *Progress in Neurobiology, 92*(4), 533–557.

Bennett, B. D., & Bolam, J. P. (1994). Synaptic input and output of parvalbumin-immunoreactive neurons in the neostriatum of the rat. *Neuroscience, 62*, 707–719.

Berns, G. S., McClure, S. M., Pagnoni, G., & Montague, P. R. (2001). Predictability modulates human brain response to reward. *Journal of Neuroscience, 21*(8), 2793–2798.

Bloch, M. H., Leckman, J. F., Zhu, H., & Peterson, B. S. (2005). Caudate volumes in childhood predict symptom severity in adults with Tourette syndrome. *Neurology, 65*(8), 1253–1258.

Bronfeld, M., Belelovsky, K., & Bar-Gad, I. (2011). Spatial and temporal properties of tic-related neuronal activity in the cortico-basal ganglia loop. *The Journal of Neuroscience : The Official Journal of the Society for Neuroscience, 31*(24), 8713–8721.

Bronfeld, M., Belelovsky, K., Erez, Y., Bugaysen, J., Korngreen, A., & Bar-Gad, I. (2010). Bicuculline-induced chorea manifests in focal rather than globalized abnormalities in the activation of the external and internal globus pallidus. *Journal of Neurophysiology, 104*(6), 3261–3275.

Bronfeld, M., Israelashvili, M., & Bar-Gad, I. (2013). Pharmacological animal models of Tourette syndrome. *Neuroscience and Biobehavioral Reviews, 37*(6), 1101–1119.

Bronfeld, M., Yael, D., Belelovsky, K., & Bar-Gad, I. (2013). Motor tics evoked by striatal disinhibition in the rat. *Frontiers in Systems Neuroscience, 7*(Sep), 50.

Brown, L. L., Smith, D. M., & Goldbloom, L. M. (1998). Organizing principles of cortical integration in the rat neostriatum: Corticostriate map of the body surface is an ordered lattice of curved laminae and radial points. *Journal of Comparative Neurology, 392*(4), 468–488.

Carmona, S., Proal, E., Hoekzema, E. A., Gispert, J. D., Picado, M., Moreno, I., et al. (2009). Ventro-striatal reductions underpin

symptoms of hyperactivity and impulsivity in attention-deficit/hyperactivity disorder. *Biological Psychiatry, 66*(10), 972–977.
Cospito, J. A., & Kultas-Ilinsky, K. (1981). Synaptic organization of motor corticostriatal projections in the rat. *Experimental Neurology, 72*, 257–266.
Costall, B., Domeney, A. M., & Naylor, R. J. (1984). Locomotor hyperactivity caused by dopamine infusion into the nucleus accumbens of rat brain: Specificity of action. *Psychopharmacology, 82*(3), 174–180.
Costall, B., & Naylor, R. J. (1975a). Mechanism of dyskinesia induction by 1-(3,4-dihydroxyphenyl) piperazine in the rat. *Neuropharmacology, 15*, 203–210.
Costall, B., & Naylor, R. J. (1975b). The behavioural effects of dopamine applied intracerebrally to areas of the mesolimbic system. *European Journal of Pharmacology, 32*(1), 87–92.
Crossman, A. R., Mitchell, I. J., Sambrook, M. A., & Jackson, A. (1988). Chorea and myoclonus in the monkey induced by gamma-aminobutyric acid antagonism in the lentiform complex. The site of drug action and a hypothesis for the neural mechanisms of chorea. *Brain, 111*, 1211–1233.
Draganski, B., Kherif, F., Klöppel, S., Cook, P. A., Alexander, D. C., Parker, G. J. M., et al. (2008). Evidence for segregated and integrative connectivity patterns in the human Basal Ganglia. *The Journal of Neuroscience : The Official Journal of the Society for Neuroscience, 28*(28), 7143–7152.
Durston, S., Tottenham, N. T., Thomas, K. M., Davidson, M. C., Eigsti, I.-M., Yang, Y., et al. (2003). Differential patterns of striatal activation in young children with and without ADHD. *Biological Psychiatry, 53*, 871–878.
Floresco, S. B., Montes, D. R., Tse, M. M. T., & van Holstein, M. (2018). Differential contributions of nucleus accumbens subregions to cue-guided risk/reward decision making and implementation of conditional rules. *The Journal of Neuroscience : The Official Journal of the Society for Neuroscience, 38*(8), 1901–1914.
François, C., Grabli, D., McCairn, K., Jan, C., Karachi, C., Hirsch, E.-C., et al. (2004). Behavioural disorders induced by external globus pallidus dysfunction in primates II. Anatomical study. *Brain : A Journal of Neurology, 127*, 2055–2070.
Freeman, R. D., Fast, D. K., Burd, L., Kerbeshian, J., Robertson, M. M., & Sandor, P. (2000). An international perspective on tourette syndrome: Selected findings from 3,500 individuals in 22 countries. *Developmental Medicine and Child Neurology, 42*(7), 436–447.
Friedman, D. P., Aggleton, J. P., & Saunders, R. C. (2002). Comparison of hippocampal, amygdala, and perirhinal projections to the nucleus accumbens: Combined anterograde and retrograde tracing study in the macaque brain. *Journal of Comparative Neurology, 450*(4), 345–365.
García, L., Cortese, S., Anderson, D., Di, A., & Xavier, F. (2015). Locomotor activity measures in the diagnosis of attention deficit hyperactivity disorder : Meta-analyses and new findings. *Journal of Neuroscience Methods, 252*, 14–26.
Giedd, J. N., Blumenthal, J., Molloy, E., & Castellanos, F. X. (2006). Brain imaging of attention deficit/hyperactivity disorder. *Annals of the New York Academy of Sciences, 931*(1), 33–49.
Gittis, A. H., Leventhal, D. K., Fensterheim, B. a, Pettibone, J. R., Berke, J. D., & Kreitzer, A. C. (2011). Selective inhibition of striatal fast-spiking interneurons causes dyskinesias. *The Journal of Neuroscience : The Official Journal of the Society for Neuroscience, 31*(44), 15727–15731.
Grabli, D., McCairn, K., Hirsch, E. C., Agid, Y., Féger, J., François, C., et al. (2004). Behavioural disorders induced by external globus pallidus dysfunction in primates: I. Behavioural study. *Brain, 127*(9), 2039–2054.
Greven, C. U., Bralten, J., Mennes, M., O'Dwyer, L., Van Hulzen, K. J. E., Rommelse, N., et al. (2015). Developmentally stable whole-brain volume reductions and developmentally sensitive caudate and putamen volume alterations in those with attention-deficit/hyperactivity disorder and their unaffected siblings. *JAMA Psychiatry, 72*(5), 490–499.
Haber, S. N. (2003). The primate basal ganglia: Parallel and integrative networks. *Journal of Chemical Neuroanatomy, 26*(4), 317–330.
Harris, K. D., Henze, D. A., Csicsvari, J., Hirase, H., & Buzsaki, G. (2000). Accuracy of tetrode spike separation as determined by simultaneous intracellular and extracellular measurements. *Journal of Neurophysiology, 84*, 401–414.
Heilbronner, S. R., Rodriguez-Romaguera, J., Quirk, G. J., Groenewegen, H. J., & Haber, S. N. (2016). Circuit-based corticostriatal homologies between rat and primate. *Biological Psychiatry*, (27), 1–14.
Heimer, L., Aiheid, G. F., de Olmos, S., Groenewegen, H. J., Haber, S. N., Harlan, R. E., & Zahm, D. S. (1997). The Accumbens: Beyond the Core-Shell Dichotomy. *Journal of Neuropsychiatry*.
Heimer, L., Zahm, D. S., Churchill, L., Kalivas, P. W., & Wohltmann, C. (1991). Specificity in the projection patterns of accumbal core and shell in the rat. *Neuroscience, 41*(1), 89–125.
Henze, D. A., Borhegyi, Z., Csicsvari, J., Mamiya, A., Harris, K. D., & Buzsaki, G. (2000). Intracellular features predicted by extracellular recordings in the hippocampus in vivo. *Journal of Neurophysiology, 84*, 390–400.
Israelashvili, M., & Bar-Gad, I. (2015). Corticostriatal divergent function in determining the temporal and spatial properties of motor tics. *The Journal of Neuroscience: the Official Journal of the Society for Neuroscience, 35*(50), 16340–16351.
Jones, D. L. L., Mogenson, G. J. J., & Wu, M. (1981). Injections of dopaminergic, cholinergic, serotoninergic and gabaergic drugs into the nucleus accumbens: Effects on locomotor activity in the rat. *Neuropharmacology, 20*(1), 29–37.
Juergens, E., Guettler, A., & Eckhorn, R. (1999). Visual stimulation elicits locked and induced gamma oscillations in monkey intracortical- and EEG-potentials, but not in human EEG. *Experimental Brain Research, 129*(2), 247–259.
Kalanithi, P. S. A., Zheng, W., Kataoka, Y., DiFiglia, M., Grantz, H., Saper, C. B., et al. (2005). Altered parvalbumin-positive neuron distribution in basal ganglia of individuals with Tourette syndrome. *Proceedings of the National Academy of Sciences of the United States of America, 102*(37), 13307–13312.
Kataoka, Y., Kalanithi, P. S. A., Grantz, H., Schwartz, M. L., Saper, C., Leckman, J. F., et al. (2010). Decreased number of parvalbumin and cholinergic interneurons in the striatum of individuals with Tourette syndrome. *The Journal of Comparative Neurology, 518*(3), 277–291.
Kelley, A. E., Baldo, B. A., Pratt, W. E., & Will, M. J. (2005). Corticostriatal-hypothalamic circuitry and food motivation: Integration of energy, action and reward. *Physiology & Behavior, 86*(5), 773–795.
Klaus, A., & Plenz, D. (2016). A low-correlation resting state of the striatum during cortical avalanches and its role in movement suppression. *Plos Biology, 14*(12), 1–30.
Koós, T., & Tepper, J. M. (1999). Inhibitory control of neostriatal projection neurons by GABAergic interneurons. *Nature Neuroscience, 2*(1097–6256), 467–472 (Print).
Kuhnen, C. M., & Knutson, B. (2005). The neural basis of financial risk taking. *Neuron, 47*(5), 763–770.
Kunzle, H. (1975). Bilateral projections from precentral motor cortex to the putamen and other parts of the basal ganglia. An autoradiographic study in Macaca fascicularis. *Brain Research, 88*, 195–209.

Kunzle, H. (1977). Projections from the primary somatosensory cortex to basal ganglia and thalamus in the monkey. *Experimental Brain Research, 30*(4), 481–492.
Kunzle, H. (1978). An autoradiographic analysis of the efferent connections from premotor and adjacent prefrontal regions (areas 6 and 9) in Macaca fascicularis. *Brain, Behavior and Evolution, 15*(3), 210–234.
Lemon, R. N. (1984). *Methods for neuronal recording in conscious animals*. New-York: Wiley.
Logothetis, N. K. (2002). The neural basis of the blood-oxygen-level-dependent functional magnetic resonance imaging signal. *Philosophical Transactions of the Royal Society of London B Biological Sciences, 357*, 1003–1037.
Logothetis, N. K. (2003). The underpinnings of the BOLD functional magnetic resonance imaging signal. *Journal of Neuroscience, 23*, 3963–3971.
Mallet, N., Micklem, B. R., Henny, P., Brown, M. T., Williams, C., Bolam, J. P., et al. (2012). Dichotomous organization of the external globus pallidus. *Neuron, 74*(6), 1075–1086.
Matsumura, M., Tremblay, L., Richard, H., & Filion, M. (1995). Activity of pallidal neurons in the monkey during dyskinesia induced by injection of bicuculline in the external pallidum. *Neuroscience, 65*, 59–70.
McCairn, K. W., Bronfeld, M., Belelovsky, K., & Bar-Gad, I. (2009). The neurophysiological correlates of motor tics following focal striatal disinhibition. *Brain : A Journal of Neurology, 132*(8), 2125–2138.
McCairn, K. W., Nagai, Y., Hori, Y., Ninomiya, T., Kikuchi, E., Lee, J.-Y., et al. (2016). A primary role for nucleus accumbens and related limbic network in vocal tics. *Neuron, 89*(2), 300–307.
McGeorge, A. J., & Faull, R. L. M. (1989). The organization of the projection from the cerebral cortex to the striatum in the rat. *Neuroscience, 29*(3), 503–537.
Mink, J. W. (2001). Basal ganglia dysfunction in Tourette's syndrome: A new hypothesis. *Pediatric Neurology, 25*, 190–198.
Mitzdorf, U. (1987). Properties of the evoked potential generators: Current source-density analysis of visually evoked potentials in the cat cortex. *International Journal of Neuroscience, 33*, 33–59.
Mogenson, G. J. G., Jones, D. D. L. D., & Yim, C. C. Y. C. (1980). From motivation to action: Functional interface between the limbic system and the motor system. *Progress in Neurobiology, 14*(2–3), 69–97.
Mogenson, G. J., & Nielsen, M. (1984). Neuropharmacological evidence to suggest that the nucleus accumbens and subpallidal region contribute to exploratory locomotion. *Behavioral and Neural Biology, 42*(1), 52–60.
Moran, A., & Bar-Gad, I. (2010). Revealing neuronal functional organization through the relation between multi-scale oscillatory extracellular signals. *Journal of Neuroscience Methods, 186*(1), 116–129.
Morgenstern, R., Mende, T., Gold, R., Lemme, P., & Oelssner, W. (1984). Drug-induced modulation of locomotor hyperactivity induced by picrotoxin in nucleus accumbens. *Pharmacology Biochemistry and Behavior, 21*(4), 501–506.
Muramatsu, S., Yoshida, M., & Nakamura, S. (1990). Electrophysiological study of dyskinesia produced by microinjection of picrotoxin into the striatum of the rat. *Neuroscience Research, 7*(4), 369–380.
Oran, Y., & Bar-Gad, I. (2018). Loss of balance between striatal feedforward inhibition and corticostriatal excitation leads to tremor. *The Journal of Neuroscience, 38*(7), 1699–1710.
Parent, A., & Hazrati, L. N. (1995). Functional anatomy of the basal ganglia. I. The cortico-basal ganglia-thalamo-cortical loop. *Brain Research Reviews, 20*, 91–127.
Peterson, B. S., Skudlarski, P., Anderson, A. W., Zhang, H., Gatenby, J. C., Lacadie, C. M., et al. (1998). A functional magnetic resonance imaging study of tic suppression in Tourette syndrome. *Archives of General Psychiatry, 55*, 326–333.
Peterson, B., Thomas, P., Kane, M. J., Scahill, L., Zhang, H., Bronen, R., et al. (2003). Basal Ganglia volumes in patients with Gilles de la Tourette syndrome. *Archives of General Psychiatry, 60*(4), 415–424.
Phillipson, O. T., & Griffiths, A. C. (1985). The topographic order of inputs to nucleus accumbens in the rat. *Neuroscience, 16*(2), 275–296.
Pogorelov, V., Xu, M., Smith, H. R., Buchanan, G. F., & Pittenger, C. (2015). Corticostriatal interactions in the generation of tic-like behaviors after local striatal disinhibition. *Experimental Neurology, 265*, 122–128.
Qiu, A., Crocetti, D., Adler, M., Mahone, E. M., Denckla, M. B., Miller, M. I., et al. (2009). Basal ganglia volume and shape in children with attention deficit hyperactivity disorder. *The American Journal of Psychiatry, 166*(1), 74–82.
Robbins, T. W., Cador, M., Taylor, J. R., & Everitt, B. J. (1989). Limbic-striatal interactions in reward-related processes. *Neuroscience and Biobehavioral Reviews, 13*(2–3), 155–162.
Schlaggar, B. L., & Mink, J. W. (2016). Movement disorders in children. *Pediatrics in Review, 24*(2), 39–51.
Swanson, C., & Kalivas, P. (2000). Regulation of locomotor activity by metabotropic glutamate receptors in the nucleus accumbens and ventral tegmental area. *Journal of Pharmacology and Experimental, 292*(1), 406–414 (Retrieved from).
Szabo, J. (1967). The efferent projections of the putamen in the monkey. *Experimental Neurology, 19*(4), 463–476.
Tarsy, D., Pycock, C. J., Meldrum, B. S., & Marsden, C. D. (1978). Focal contralateral myoclonus produced by inhibition of GABA action in the caudate nucleus of rats. *Brain : A Journal of Neurology, 101*(1), 143–162.
Tunstall, M. J., Oorschot, D. E., Kean, A., & Wickens, J. R. (2002). Inhibitory interactions between spiny projection neurons in the rat striatum. *Journal of Neurophysiology, 88*(3), 1263–1269.
Vinner, E., Israelashvili, M., & Bar-Gad, I. (2017). Prolonged striatal disinhibition as a chronic animal model of tic disorders. *Journal of Neuroscience Methods, 292*, 20–29.
Voorn, P., Gerfen, C. R., & Groenewegen, H. J. (1989). Compartmental organization of the ventral striatum of the rat: Immunohistochemical distribution of enkephalin, substance P, dopamine, and calcium-binding protein. *Journal of Comparative Neurology, 289*(2), 189–201.
Wachtel, H., Anden, N. E., Helmut, W., & Nils-Erik, A. (1978). Motor activity of rats following intracerebral injections of drugs influencing GABA mechanisms. *Archive of Pharmacology, 302*, 133–139.
Wong, L. S., Eshel, G., Dreher, J., Ong, J., & Jackson, D. M. (1991). Role of dopamine and GABA in the control of motor activity elicited from the rat nucleus accumbens. *Pharmacology Biochemistry and Behavior, 38*(4), 829–835.
Worbe, Y., Baup, N., Grabli, D., Chaigneau, M., Mounayar, S., McCairn, K., et al. (2009). Behavioral and movement disorders induced by local inhibitory dysfunction in primate striatum. *Cerebral Cortex, 19*(8), 1844–1856.
Worbe, Y., Sgambato-Faure, V., Epinat, J., Chaigneau, M., Tandé, D., François, C., et al. (2013). Towards a primate model of Gilles de la Tourette syndrome: Anatomo-behavioural correlation of disorders induced by striatal dysfunction. *Cortex, 49*, 1126–1140.
Wu, M., Brudzynski, S. M., & Mogenson, G. J. (1993). Functional interaction of dopamine and glutamate in the nucleus

accumbens in the regulation of locomotion. *Canadian Journal of Physiology and Pharmacology, 71*(5–6), 407–413.

Yael, D., Israelashvili, M., & Bar-Gad, I. (2016). Animal models of tourette syndrome-from proliferation to standardization. *Frontiers in Neuroscience, 10*, 1–6.

Yael, D., Tahary, O., Gurovich, B., Belelovsky, K., & Bar-Gad, I. (2019). Disinhibition of the nucleus accumbens leads to macro-scale hyperactivity consisting of micro-scale behavioral segments encoded by striatal activity. *The Journal of Neuroscience : The Official Journal of the Society for Neuroscience, 39*(30), 5897–5909.

Yael, D., Zeef, D. H., Sand, D., Moran, A., Katz, D. B., Cohen, D., et al. (2013). Haloperidol-induced changes in neuronal activity in the striatum of the freely moving rat. *Frontiers in Systems Neuroscience, 7*, 110.

Yoshida, M., Nagatsuka, Y., Muramatsu, S., & Niijima, K. (1991). Differential roles of the caudate nucleus and putamen in motor behavior of the cat as investigated by local injection of GABA antagonists. *Neuroscience Research, 10*(1), 34–51.